Thermal Dissociation and H_2S Reactivity of Czech Limestones

M. HARTMAN*, O. TRNKA, K. SVOBODA, and V. VESELÝ

Institute of Chemical Process Fundamentals, Academy of Sciences of the Czech Republic, CZ-165 02 Prague
e-mail: hartman@icpf.cas.cz

Received 11 June 2002

A differential reactor with a fixed bed of limestone/calcine particles was employed to measure their conversion to calcium oxide/calcium sulfide as mass loss/gain. The overall rate of sulfidation was found to be affected strongly by the particle size and by the conversion of calcium oxide to calcium sulfide. The obtained experimental data indicate that strong diffusional resistances develop in the interior of particles in the course of the sulfidation. The conversions of calcines from eight different, commercially exploited limestones were explored: their ultimate values are fairly high and different. The differences cannot be related to the differences in chemical composition of the rocks. The overall genesis of the limestone rocks appears to play an important role in developing their reactivity towards H_2S.

Coal maintains its principal use in electric power generation. However, the environmental issues related to this technology might potentially limit its use and effectiveness.

The so-called integrated gasification combined cycle (IGCC) provides a promising way of generating power from coal. At first, coal is gasified by means of air, O_2, and/or water vapour to produce a concentrated raw coal (fuel) gas. After its clean-up, the coal gas fires a gas turbine. The hot flue gas from the gas turbine passes through a boiler to generate steam that is then employed to drive a steam turbine. It is envisaged that the IGCC technology can attain power-generation efficiencies as high as 52 % [1].

In the reducing conditions of gasification, sulfur contained in the coal is converted predominantly into H_2S. COS (carbonyl sulfide) and CS_2 (carbon disulfide) are the secondary sulfur species occurring in raw coal gas [2, 3]. The clean-up of gas is necessary not only for the protection of the gas turbine, but also to comply with the stringent environmental regulations. In order to maintain the overall high efficiency of the process, coal gas needs to be cleaned at high temperature. Coal gas desulfurization to sufficiently low levels of H_2S at temperatures above 600 ℃ and at pressures of 1—3 MPa is generally recognized as a crucial step in the designed IGCC systems. According to the latest estimates, a reduction of the H_2S concentration down to 20 vol. ppm is needed, corresponding to H_2S partial pressure of 60 Pa at a total pressure of 3 MPa [4].

Thermodynamic calculations suggest that the oxides of metals such as Zn, V, Ca, and Mn exhibit strong affinity to H_2S at high temperature [5]. However, it should be noted that Zn vaporizes at temperatures higher than 700 ℃ and V_2S_3 melts at about 650 ℃. CaO-Based sorbents are effective under both reducing and oxidizing conditions. It is thus expected that high-temperature removal of at least the bulk of H_2S from coal gas can be attained using inexpensive limestone- or dolomite-derived sorbents. Calcium sulfide forms in the reducing milieu, calcium sulfate is formed in the oxidizing environments. Thermodynamic calculations reveal that very little or none of the magnesium in dolomite materials ($CaCO_3 \cdot MgCO_3$) can combine with H_2S or COS at elevated temperature [6].

Spent sulfided lime/limestone can be used as a building material after oxidation towards sulfate (gypsum) or as a fluxing agent in entrained flow coal gasifiers. As essentially inert, $CaSO_4$ can be disposed of in landfill sites. Regeneration of the spent sorbent is not a straightforward operation. Sulfided limestone calcines can be regenerated with steam and CO_2 or by partial oxidation with SO_2 to elemental sulfur and calcium sulfate combined with subsequent reaction between remaining CaS and $CaSO_4$ at high temperature [4, 7].

The kinetics of the reaction between hydrogen sulfide and limestone- or dolomite-based materials has been a subject of research for some years. Practically all investigators report the rates of sulfidation being high enough to make it possible to use CaO-sorbents for coal gas desulfurization on a practical scale. For a review of the literature on sulfidation kinetics, the reader is referred to a recent work of ours [8].

*The author to whom the correspondence should be addressed.

The wide variation in H_2S reactivity of different naturally occurring rocks appears to be a major factor in the development of limestone/dolomite-based processes for H_2S removal. This experimental study explores the reactivity (performance) and pore structure of the calcined specimens originated from parent carbonate rocks of different geological types.

THEORETICAL

The content of H_2S in coal gas can be reduced to low values according to the reaction

$$CaO(s) + H_2S(g) \leftrightarrow CaS(s) + H_2O(g) \qquad (A)$$

$$\Delta_r H^o_{(A)}(298\ K) = -59.44\ kJ\ mol^{-1}$$

It is assumed that the transitory intermediate Ca(OH)(SH) is formed in the course of overall reaction (*A*) [8]. Although H_2S can also react with limestone ($CaCO_3$), a prerequisite for its rapid removal from the gaseous phase is the occurrence of its calcine (CaO, lime) in the system. A fundamental difference between the reaction of H_2S with lime and that with limestone is the presence of an alkaline, highly developed porous structure within the reacting lime particles.

In order to eliminate possible hindrance effects of the CO_2 also present in coal gas, reaction (*A*) must occur above the temperatures expressed by the equilibrium relationship

$$T/K \geq 20007.43/(21.68602 - \ln(p(CO_2)/kPa)) \quad (1)$$

We deduced eqn (*1*) from the experimental measurements of *Johnston* [9] in our recent work [10].

The equilibrium state of reaction (*A*) is inherently independent of pressure and can be described by the equation

$$\ln[\varphi(H_2O)/\varphi(H_2S)] = 7258.685\ K/T + 0.103379 \quad (2)$$

where $\varphi(H_2O)$ and $\varphi(H_2S)$ signify the volume fractions of water vapour and hydrogen sulfide, respectively [6]. It is apparent that maximum potential of H_2S removal occurs precisely at the calcination temperature of calcium carbonate, which is the function (*1*) of the partial pressure of carbon dioxide.

For a specified total pressure and H_2O and CO_2 contents in the gas, the equilibrium content of H_2S at the calcination temperature of $CaCO_3$ is then expressed by

$$\varphi(H_2S) = 3.4531 \times 10^{-4}\varphi(H_2O) \cdot \cdot (\{\varphi(CO_2)\}(p/kPa))^{0.3628} \qquad (3)$$

where p is the total pressure in the system given in kPa.

Provided that the industrial process operates at 2 MPa with a gas containing 2 vol. % CO_2 and 2 vol. % H_2O, eqn (*3*) estimates that the equilibrium content of H_2S amounts to about 26 vol. ppm. According to eqn (*1*), the calcination temperature in this system is as large as approximately 839 °C. Contact between solid and gas can readily be attained by passing coal gas through a packed, moving or fluidized bed of lime particles [11].

The predictions of eqn (*3*) suggest that the use of CaO might not always meet the stringent process requirements in all cases. However, because of its low cost, it can be economically attractive to employ lime for removal of the bulk of the H_2S (and COS) from coal gas, utilizing a more efficient (and more expensive) sorbent, such as that based on Zn, in the subsequent polishing step.

EXPERIMENTAL

Eight different limestone rocks from various quarries, located throughout Bohemia and Moravia, were employed in this study as listed in Table 1. Their hand-picked samples without visible inclusions were

Table 1. Chemical Analyses of Limestones

Limestone	w_i/mass %						Porosity of calcine[c] (calcined at 900 °C)
	CaO[a]	MgO	SiO_2	Al_2O_3	Fe_2O_3	Mass loss on ignition[b] at 900 °C	
CD	54.6	0.42	1.00	0.15	0.11	42.9	0.480
CI	42.4	0.63	15.01	3.57	1.40	35.3	0.461
LA	32.8	18.84	1.09	0.29	0.24	45.8	0.530
ME	54.9	0.06	0.35	0.12	0.20	43.1	0.500
MO	54.9	0.42	0.27	0.09	0.11	43.4	0.527
PR	53.2	1.57	0.47	0.26	0.22	43.5	0.507
ST	53.6	0.73	2.15	0.54	0.47	42.4	0.518
VI	55.0	0.21	0.29	0.10	0.08	43.1	0.512

a) The value for a pure carbonate (100 % $CaCO_3$) is as large as 56.028 mass %. *b*) The stoichiometry provides a value of 43.972 mass %. *c*) Determined by helium and mercury displacement. The theoretical value for the pure and nonporous parent $CaCO_3$ (calcite) amounts to 0.54197.

subjected to mineralogical as well as chemical analyses. The mineralogical analyses were made by X-ray diffraction. They revealed that apart from sample LA, the primary component of the rocks was calcite (hexagonal with rhombohedral structures). The presence of aragonite, which is orthorhombic, was not detected. Dolomite was the main and calcite was the minor component of sample LA. Carbonates were white or whitish with various shades of grey, yellow or pink. All the rocks were crystalline, with average grain sizes ranging from about 30 μm to 1 mm. Among minor or rather trace components, there were quartz, clay, sericite, and organic residues. Under a microscope, the irregular shape of the crushed and sieved particles was clearly noticeable. In general, the solids exhibited sharp edges and, quite often, smooth crystalline surfaces could be seen. Except for rock CI, all the samples were virtually nonporous in the natural state. The porosity of carbonate sample CI amounted to a few percent.

In the samples collected, the following components were determined: CaO, MgO, SiO_2, Al_2O_3, Fe_2O_3, and the mass loss on ignition. The results of the chemical analyses are given in Table 1. Based on the $CaCO_3$ content, six of the eight carbonate rocks examined can be classified as high-calcium or chemical-grade limestones since they contain more than 95 mass % $CaCO_3$ [12]. Sample LA is classified as strongly dolomitic limestone (58.5 mass % $CaCO_3$, 39.4 mass % $MgCO_3$). With respect to its texture, rock CI is considered as mudstone carbonate. Aside from its lower content of $CaCO_3$ (75.7 mass %), it is of interest to note the considerable portion of SiO_2 (15 mass %) as well as the appreciable presence of Al_2O_3 (3.6 mass %) and Fe_2O_3 (1.4 mass %).

The hand-picked samples were crushed and sieved and the fractions of particles within size ranges 0.25—0.32 mm ($\bar{d}_p = 0.285$ mm), 0.50—0.63 mm ($\bar{d}_p = 0.565$ mm), and 1.00—1.25 mm ($\bar{d}_p = 1.12$ mm) were used as precursor (parent) solids.

Decomposition experiments were conducted at a constant rate of temperature increase in the conventional thermogravimetric analysis equipment (Perkin—Elmer) at a slow heating rate of 3 ℃ min^{-1}. To reduce the possibility of heat-transfer and mass-transfer effects, sample masses were close to 15 mg and nitrogen flow of 70 cm^3 min^{-1} was maintained through the gas space to ward off the gaseous product of the reaction. The size of the sample used was judged to be a reasonable compromise between heat- and mass-transfer intrusions and a relative error in mass measurement. Such conditions ensure that heat- and mass-transfer effects are minimized with intraparticle sample temperature gradients less than 2—4 ℃.

Fractional conversions were calculated from the decrease in sample mass, $m_o - m(\tau)$, at any time and the equation

$$X_C = [M_{CaCO_3}/(M_{CO_2} w(CaCO_3))] \cdot [m_o - m(\tau)]/m_o \quad (4)$$

where $w(CaCO_3)$ is the mass fraction of calcium carbonate in the original sample and M_i is the molar mass of species. Complete theoretical conversion ($X_C = 1$, $w(CaCO_3) = 1$) corresponds to the mass loss $\Delta m/m_o = 0.43972$.

In larger samples, calcined in a differential reactor, physical properties such as pore size distribution, pore (void) volume, and BET specific surface area were determined [13, 14]. Porosities of the samples were determined by helium and mercury displacement. Pore size distributions were determined by measuring the volume of mercury penetrating the pore volume at increasing pressure using a Micromeritics porosimeter.

Reaction between CaO and H_2S (A) was explored at atmospheric pressure and constant temperature using a high-temperature, differential reactor with the fixed bed of particles described earlier [13, 14]. To ensure that the measured reaction rates were not affected by mass transfer to the surface of solids, a high flow rate of gas was employed in each experiment (2.5 m s^{-1}). Very small changes in the gas composition (to approximate "differential conditions") were realized by using small samples (about 15 mg) of precalcined limestone particles. Larger samples were used for a porosity study in which the rate of reaction was not determined. The gas entering the differential reactor contained 0.35 vol. % H_2S, 1 vol. % H_2, 2 vol. % CO_2, and 5 vol. % water vapour, the balance being nitrogen. Predictions of eqn (*1*) suggest that no CO_2 from this gas mixture can combine with CaO at temperatures above 681 ℃, and hence only CaS is formed in such conditions.

To suppress a potential depletion of H_2S, we supplied hydrogen to the sulfidation gas. The residence time of gas in the reactor tube was as short as less than 0.5 s. The addition of carbon monoxide to the reactant gas prevents undesirable oxidation of CaS to $CaSO_4$ with CO_2. For the issue of possible side reactions, the reader is referred to a recent study of ours [8].

Fractional conversions were calculated from the increase in the sample mass due to the sulfidation reaction (A), $m(\tau) - m_o$, at any time, τ, and the equation

$$X = \{M_{CaO}/[(M_{H_2S} - M_{H_2O}) w(CaO)]\} \cdot \cdot [m(\tau) - m_o]/m_o \quad (5)$$

where $w(CaO)$ is the mass fraction of CaO in the original sample (calcine) and M_i is the molar mass of species i. X-Ray diffraction analyses confirmed that CaS is formed exclusively in the samples of reacted solids withdrawn after sulfidation. Complete theoretical conversion ($X = 1$, $w(CaO) = 1$) corresponds to the mass increase $\Delta m/m_o = 0.28652$.

The samples of calcines for the sulfidation were pre-

pared by thermal decomposition of suitable fractions of the carbonates carried out for 2 h at 850 ℃ in an electric muffle furnace under slow flow of air as a sweep gas. The calcined particles were carefully sieved again, and the narrow fractions of calcines were maintained in airtight containers. The irregular shape of the solids was not changed substantially by the process of calcination. Our experience indicates that under the above mild conditions of calcination the sintering process of CaO is of little relevance.

RESULTS AND DISCUSSION

Thermogravimetric analysis provides the data which can serve as a basis for describing the decomposition kinetics under well controlled laboratory conditions. Although extreme care is taken in the experimental work to reduce all presumable side effects, the results obtained are only approximate.

The TGA data indicated that the calcination of sample VI became noticeable at about 660 ℃. The temperature was increased at a rate of 3 ℃ min^{-1} to a final temperature of approximately 830 ℃ where decomposition of calcium carbonate to calcium oxide was practically complete.

Experience shows that the thermal decompositions of solids can often be described by the following rate law [15, 16]

$$\mathrm{d}X_\mathrm{C}/\mathrm{d}\tau = k_\mathrm{o}(1 - X_\mathrm{C})^n \exp(-E/RT) \qquad (6)$$

with the initial condition $X_\mathrm{C}(0) = X_\mathrm{i}$ and where k_o is the preexponential factor, E is the apparent activation energy, X_C is the fractional conversion of the decomposing carbonate to oxide given by eqn (*4*), and n is the apparent order of the reaction. Eqn (*6*) is a convenient basis for correlation since it subsumes most of the prior nucleation and diffusion models [17].

The experimental data accumulated from the temperature increase run were tested empirically by fitting to eqn (*6*). Thirty data points at equal temperature intervals were taken to fit this equation. The derivatives $\mathrm{d}X_\mathrm{C}/\mathrm{d}\tau$ were approximated as $\Delta X_\mathrm{C}/\Delta\tau$ and estimated from the conversion measured as a function of time and temperature. The values of the kinetic parameters were computed by the simplex procedure (flexible polyhedron search), using appropriate statistical evaluations for estimating the confidence intervals of the sought parameters.

The computed apparent energy of activation, E, is as large as 264.09 kJ mol^{-1}. The estimated apparent order of reaction is $n = 0.6667$, and the preexponential factor (frequency factor) amounts to $k_\mathrm{o} = 1.3324 \times 10^{11}$ s^{-1}. The relative standard deviation was ±8 %.

The rate of calcination of the fine-ground carbonate samples VI was also measured in the constant temperature mode. The predictions of eqn (*6*) with the above fitted parameters are compared to the constant

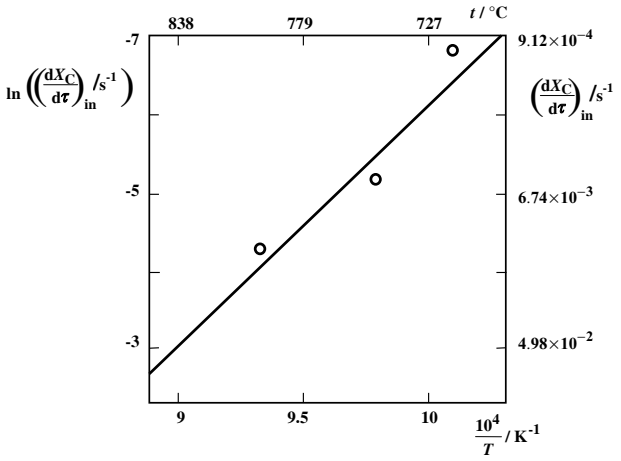

Fig. 1. Initial rates of the calcination of sample VI at different temperatures: O – constant temperature data. The straight line shows predictions of eqn (*6*) with the reaction parameters deduced from the temperature increase experimental data.

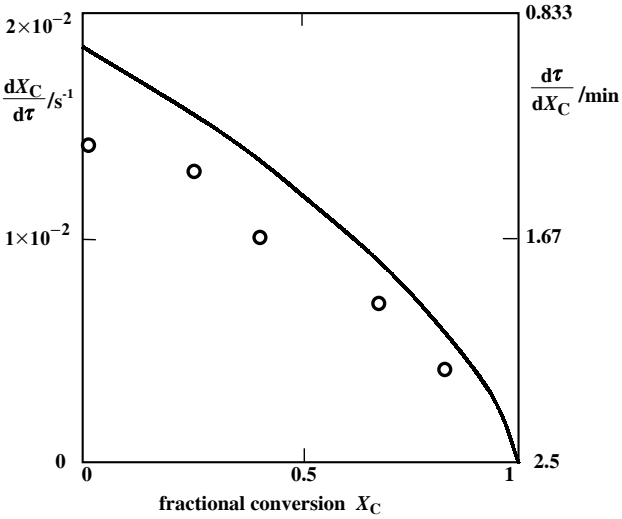

Fig. 2. Dependence of the calcination reaction rate on the conversion of calcium carbonate at 800 ℃. The symbols are the same as in Fig. 1.

temperature data in Figs. 1 and 2. As can be seen, there is reasonably good agreement between the results amassed by the different modes of experiments.

The obtained TGA results are in good agreement with our previous results. Having worked with submillimeter-size particles of limestones, we found that their calcination was complete within 2—3 min at temperatures near/above 800 ℃. However, it should be reminded that the calcination reaction

$$\mathrm{CaCO_3(s)} \rightarrow \mathrm{CaO(s)} + \mathrm{CO_2(g)} \qquad (B)$$

$$\Delta_\mathrm{r}H^\mathrm{o}_{(\mathrm{B})}(298\ \mathrm{K}) = +178.53\ \mathrm{kJ\ mol^{-1}}$$

is strongly endothermic. It is apparent that any deeper insight, particularly into the thermal dissociation of larger particles, must include the rate of heat transfer to the reaction interface (zone) as well as the rate of transport of CO_2 from this zone.

Calcium carbonate undergoes deep transformations during its calcination. In the course of heating (burning), the original rhombohedral structure of calcium carbonate changes into the cubic crystal structure of calcium oxide. In difference to the crystalline parent limestones, the calcines appear to be amorphous to the unaided eye. X-Ray diffraction analyses indicate, however, that all calcines (quicklimes) are microcrystalline.

The decomposition of calcium carbonate produces a porous (spongy texture) calcium oxide the pore volume and surface area of which are far greater than those of the precursor stone. Smaller part of the porosity of lime particles, e_C, arises from the porosity of the parent carbonate rock, e_{LS}, while the major part comes from the progress of the decomposition process (X_C) [18, 19]

$$e_C = 1 - (1 - e_{LS}) \cdot \{1 + (\rho_{LS}/\rho_{CaCO_3}) w(CaCO_3) \cdot \cdot [(V_{CaO} - V_{CaCO_3})/V_{CaCO_3}] X_C\} \quad (7)$$

The symbols V_i in eqn (7) denote the molar volumes of the respective species ($V_{CaCO_3} = 36.93$ cm^3 mol^{-1} and $V_{CaO} = 16.92$ cm^3 mol^{-1}) and $w(CaCO_3)$ is the mass fraction of $CaCO_3$. When the numerical values for V_i are incorporated into this equation, we can see that the porosity of the lime, e_C, produced by calcination of nonporous crystals of pure calcite ($e_{LS} = 0$, $\rho_{LS} = \rho_{CaCO_3}$, $w(CaCO_3) = 1$, and $X_C = 1$) is as high as 0.5420.

Assuming $\rho_{LS} = \rho_{CaCO_3}$ and $e_{LS} = 0$ for the examined high-calcium crystalline limestones from Table 1, the porosities of the calcined limestones predicted by eqn (7) range from 0.510 to 0.535. Thus, the experimental (Table 1) and theoretical porosities of the calcines are in satisfactory agreement. The somewhat lower experimental values suggest that slight shrinkage of the decomposing particles cannot be ruled out.

The porosity distribution curve that was determined for calcined sample VI from the mercury porosimetry results, is shown in Fig. 3. Curve *1* in this figure indicates that the radii of pores are distributed over the 10—1000 nm range. The most probable pore radius of the VI calcine, which is the point where a sharp increase in the pore volume occurs, is approximately 60 nm.

In addition to the porosity and pore size distribution, the specific surface area (BET) of the calcines was determined as well. The measured values were in the range 1.5—4.8 m^2 g^{-1}. It should be pointed out that the calcines (CaO) possess a far greater porosity and surface area than the parent carbonates. Moreover, the CaO surface is strongly alkaline in stark contrast to the entirely neutral surface of the carbonate precursors. Consequently, a few degrees above the calcination point – given by eqn (*1*) – calcines (limes) are far more reactive (efficient) sorbents than are limestones a few degrees below the calcination point. Our experience indicates that the sintering (or degradation) of the textural parameters of the calcines is of little practical importance at temperatures below 950 °C.

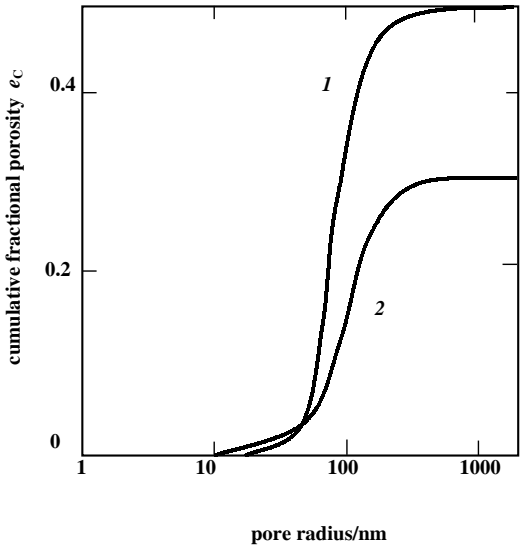

Fig. 3. Pore size distribution of calcine VI produced at 850 °C (curve *1*), and calcine VI sulfided at 750 °C for 50 min (curve *2*).

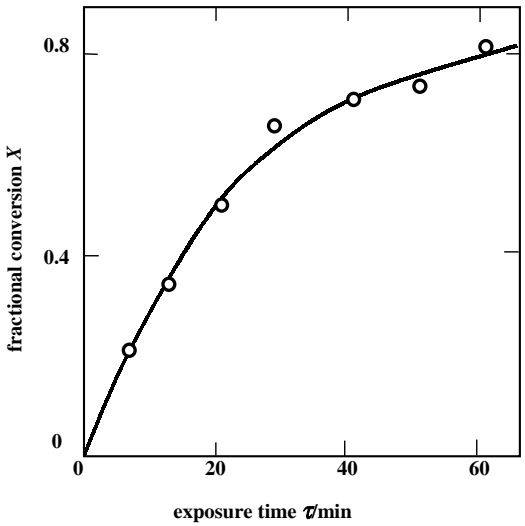

Fig. 4. Dependence of the conversion of calcium oxide to sulfide on the exposure time: temperature 750 °C; concentration of H_2S 0.35 vol. %; particle size $\bar{d}_p = 0.565$ mm; calcine VI.

As to be expected, the rate of sulfidation of CaO increases with temperature (700—800 °C) and at increasing H_2S concentrations (0.12—0.51 vol. % H_2S). It is obvious from the results presented in Fig. 4 that

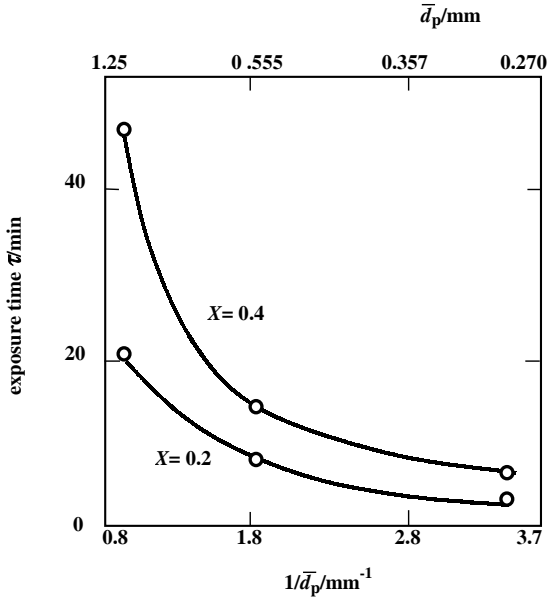

Fig. 5. Effect of particle size on the exposure (reaction) time needed to attain given conversions of calcine VI at 750 °C with 0.35 vol. % H_2S in the gas phase.

the sulfidation reaction is rapid in its initial stage. As the exposure time goes on, however, the rate of reaction decreases appreciably. While the initial rate of sulfidation suggests that all CaO might be completely converted to CaS in about 30 min of exposure, a conversion of 80 % was attained after 60 min.

Three fractions of calcine particles within sieve size ranges 0.25—0.32 mm ($\bar{d}_p$ = 0.285 mm), 0.50—0.63 mm ($\bar{d}_p$ = 0.565 mm), and 1.00—1.25 mm ($\bar{d}_p$ = 1.12 mm) were used to determine the effect of the particle size on the conversion at 750 °C. Reactivity evolution data were amassed in the form of markedly concave conversion *vs.* exposure time curves that were similar to the dependence shown in Fig. 4. Using such curves, we estimated the exposure times needed to achieve the conversions 20 % and 40 %, respectively. The results presented in Fig. 5 clearly demonstrate the appreciable influence of particle size on the overall rate of the CaO-H_2S reaction. This indicates that there are strong intraparticle diffusional intrusions into the overall reaction process. Fig. 3 visualizes the pronounced effect of the sulfidation on the pore size distribution and porosity of the reacting particles. As can be seen in this figure, there is a shift of the most probable pore size because of the sulfidation. More important is the reduction in porosity of particles from 50.7 % to 30 % caused by the progress of the sulfidation reaction from zero to about 75 %. Even though the crystal structures of both the reactant calcium oxide and the product calcium sulfide are cubic, their molar volumes are notably different (V_{CaO} = 16.92 cm^3 mol^{-1} and V_{CaS} = 28.86 cm^3 mol^{-1}). Assuming that the physical dimensions of a particle do not change during the reaction and conditions are uniform throughout the interior of the particle, then from a mass balance on the volume of the solid phase, the following relationship can be written between the conversion, X, and the void fraction, e_X

$$e_X = 1 - (1 - e_C) \cdot \{1 + (\rho_C/\rho_{CaO}) w(CaO) \cdot \cdot [(V_{CaS} - V_{CaO})/V_{CaO}] X\} \quad (8)$$

Provided that $\rho_C = \rho_{CaO}$, $\rho_{LS} = \rho_{CaCO_3}$, $w(CaO) = w(CaCO_3) = 1$, ($X_C = 1$), and $e_{LS} = 0$, then on combining eqns (*7*) and (*8*), we can simply express the porosity of such a sulfided particle as

$$e_X = 1 - [V_{CaO} + (V_{CaS} - V_{CaO})X]/V_{CaCO_3} \quad (9)$$

Introducing the V_i values, we can see that the rate at which the volume of the solid phase increases with the progress of the sulfidation is as follows

$$dV_S/dX = (V_{CaS} - V_{CaO})/V_{CaCO_3} = 0.3234 \quad (10)$$

Such accumulation and growth of the reaction product within the porous structure appears to be the underlying cause of the continuous decrease in the reaction rate as shown in Fig. 4. The concave shape of the curve in this figure suggests a notable build-up of diffusional resistances in the interior of particles in the course of the reaction.

Eqn (*9*) also predicts that the calcine of a nonporous parent limestone remains quite porous (e_X = 0.2186), even when all CaO is converted to CaS (*i.e.* $X = 1$). This suggests that the interior of the reacted particle of calcine is accessible for H_2S until all CaO is depleted. As visualized in Fig. 4 and as our general experience with the sulfidation reaction indicates, high conversions can be attained, particularly with smaller particles.

However, the strong effect of particle size on the overall rate of sulfidation clearly manifests that strong intraparticle diffusional resistances develop as the sulfidation proceeds. As seen in Fig. 5, the average overall rate of sulfidation considerably decreases with the increasing particle size. The curves in this figure were deduced from the conversion *vs.* exposure time results during the sulfidation at 750 °C. For example, the conversion of 40 % was achieved with the 0.285 mm particles after the exposure for 7 min. Enlarging the particles by the factor of about four ($\bar{d}_p$ = 1.12 mm) increases the needed exposure time to approximately 50 min (50 min/7 min = 7.1). It might be interesting to note that the relative changes in exposure time are practically identical for both conversions (20 % and 40 %).

Nine different, commercially exploited limestone rocks from various deposits located throughout Bohemia and Moravia were selected for this research. One of the specimens was found to decrepitate

Table 2. Ultimate Conversions of the Limestone Calcines[a]

Parent limestone	$w(CaCO_3)$	Ultimate X	Specific consumption (limestone mass per 1 g of sulfur)/g[b]
CD	0.975	0.646	4.96
CI	0.757	0.968	4.26
LA	0.585	0.974	5.47
ME	0.980	0.770	3.97
MO	0.980	0.662	4.81
PR	0.950	0.699	4.70
ST	0.957	0.737	4.43
VI	0.982	0.852	3.73

a) Temperature 750 °C; particle size 0.565 mm; content of H_2S 0.35 vol. %; duration of exposure to the reactant gas 90 min. *b*) The stoichiometric value is 3.121 g of $CaCO_3$.

severely upon heating and, therefore, it was not employed in further work. Conversions of eight different calcined stones with 0.565 mm particles exposed at 750 °C for 90 min to the simulated coal gas containing 0.35 vol. % H_2S are given in Table 2. The attained ultimate conversions are considerably high and range from 0.65 to 0.97. It should be noted, however, that the highest conversions were reached with the samples containing the lowest fractions of CaO. Having in mind the differences in contents of the active component (CaO), the specific consumption of limestone as a practical parameter is also employed in Table 2 aside to the conversion. The chemical composition does not explain the wide variation in the ultimate conversion (reactivity) of the calcines, and their porosities are not much different. As shown in Table 2, calcines VI and ME appear as the most effective H_2S scavengers in terms of the specific consumption of the parent carbonate. Independent X-ray diffraction study indicated that both precursors of calcines VI and ME were of a very fine-grained structure.

By means of the electron microprobe, the sulfur distribution was determined within individual particles. The analyses show that the sulfidation proceeds throughout the whole interior of the reacted particles. Nevertheless, there seems to be a tendency to an appreciable enrichment with sulfur at the outer edge of the particles.

CONCLUSION

Particles of limestone smaller than about 1 mm decompose rapidly at temperatures above 750—800 °C. An extensive pore structure gradually develops during the calcination of virtually nonporous, natural carbonate rocks.

The sulfidation reaction is fast in its initial stage. However, as the reaction continues, both the porosity of the reacting particles and the rate of sulfidation notably decrease. Appreciable diffusional resistances build up within the interior of particles in the course of the sulfidation.

The ultimate conversions of calcined specimens of eight commercial limestones are fairly high. The differences in conversion cannot be related to differences in chemical composition of the samples. Although the sulfidation reaction takes place throughout the whole volume of reacting particles, their outer zones are enriched with sulfur.

Acknowledgements. The authors wish to express their thanks to the Grant Agency of the Academy of Sciences of the Czech Republic (Grant No. A 4072201) and the Grant Agency of the Czech Republic (Grant No. 203/02/0002) for their financial support.

SYMBOLS

$\bar{d}_p$	average particle size determined by sieving	mm
dV_S/dX	rate of increase in the relative volume of solid phase given by eqn (*10*)	
$dX_C/d\tau$	rate of conversion of calcium carbonate to calcium oxide	s^{-1}
$(dX_C/d\tau)_{in}$	initial rate of conversion of calcium carbonate to calcium oxide at $X_C \to 0$	s^{-1}
$\Delta_r H^o_{(i)}$ (298 K)	standard enthalpy of reaction i at 298 K	kJ mol^{-1}
e_C	fractional porosity of a completely calcined particle (CaO, calcine, lime)	
e_{LS}	fractional porosity of natural carbonate rock	
e_X	fractional porosity of a sulfide-loaded particle	
E	effective (apparent) activation energy	kJ mol^{-1}
k_o	Arrhenius constant	s^{-1}
M_{CaCO_3}	molar mass of calcium carbonate = 100.087	g mol^{-1}
M_{CaO}	molar mass of calcium oxide = 56.077	g mol^{-1}
M_{CO_2}	molar mass of carbon dioxide = 44.010	g mol^{-1}
M_{H_2O}	molar mass of water = 18.015	g mol^{-1}
M_{H_2S}	molar mass of hydrogen sulfide = 34.082	g mol^{-1}
n	apparent order of reaction	

$p(CO_2)$	partial pressure of carbon dioxide	kPa
p	operation (total) pressure	kPa
R	ideal gas-law constant = 8.31441 J (mol K)$^{-1}$	
T	thermodynamic temperature	K
t	Celsius temperature	°C
V_{CaCO_3}	molar volume of calcium carbonate = 36.932	cm^3 mol^{-1}
V_{CaO}	molar volume of calcium oxide = 16.916	cm^3 mol^{-1}
V_{CaS}	molar volume of calcium sulfide = 28.858	cm^3 mol^{-1}
V_s	fractional volume of solid phase in the particle = $1 - e_X$	
m_o	original (initial) mass of the sample	g
$m(\tau)$	mass of the reacted sample at moment of time τ	g
X	fractional conversion of calcium oxide to calcium sulfide	
X_C	fractional conversion of calcium carbonate to calcium oxide	
$w(CaO)$	mass fraction of calcium oxide	
$w(CaCO_3)$	mass fraction of calcium carbonate	

Greek Letters

ρ	true (skeletal, helium) density	g cm^{-3}
ρ_C	density of calcine	g cm^{-3}
ρ_{CaCO_3}	density of calcite = 2.710	g cm^{-3}
ρ_{CaO}	density of calcium oxide = 3.315	g cm^{-3}
ρ_{CaS}	density of calcium sulfide = 2.500	g cm^{-3}
ρ_{LS}	density of limestone rock	g cm^{-3}
τ	elapsed time of reaction	s
$\varphi(CO_2)$	volume fraction of carbon dioxide	
$\varphi(H_2O)$	volume fraction of water vapour	
$\varphi(H_2S)$	volume fraction of hydrogen sulfide	

REFERENCES

1. Chauk, S. S., Agnihotri, R., Jadhav, R. A., Misro, S. K., and Fan, L.-S., *AIChE J. 46*, 1157 (2000).
2. Hartman, M., Svoboda, K., Trnka, O., and Veselý, V., *Chem. Listy 93*, 315 (1999).
3. Hartman, M., Svoboda, K., and Trnka, O., *Collect. Czech. Chem. Commun. 64*, 157 (1999).
4. van der Ham, A. G. J., Heesink, A. B. M., Prins, W., and van Swaaij, W. P. M., *Ind. Eng. Chem. Res. 35*, 1487 (1996).
5. Hartman, M., Svoboda, K., Trnka, O., and Veselý, V., *Chem. Listy 93*, 99 (1999).
6. Hartman, M., Trnka, O., and Svoboda, K., *Acta Montana IRSM AS CR, Ser. B*, No. 9 (112), 5 (1999).
7. Adánez, J., García-Labiano, F., Abad, A., de Diego, L. F., and Gayán, P., *Energy Fuels 15*, 85 (2001).
8. Hartman, M., Svoboda, K., Trnka, O., and Čermák, J., *Ind. Eng. Chem. Res. 41*, 2392 (2002).
9. Johnston, J., *J. Am. Chem. Soc. 32*, 938 (1910).
10. Hartman, M., Svoboda, K., and Trnka, O., *Chem. Pap. 54*, 302 (2000).
11. Yates, J. G., *Fundamentals of Fluidized-Bed Processes.* Butterworths, London, 1983.
12. Oates, J. A. H., *Lime and Limestone.* Wiley—VCH, Weinheim, 1998.
13. Hartman, M. and Trnka, O., *AIChE J. 39*, 615 (1993).
14. Hartman, M., Trnka, O., and Veselý, V., *AIChE J. 40*, 536 (1994).
15. Mu, J. and Perlmutter, B. D., *Thermochim. Acta 49*, 207 (1981).
16. Hartman, M., Trnka, O., Veselý, V., and Svoboda, K., *Chem. Eng. Commun. 185*, 1 (2001).
17. Mu, J. and Perlmutter, D. D., *Ind. Eng. Chem., Process Des. Dev. 20*, 640 (1981).
18. Hartman, M. and Coughlin, R. W., *Ind. Eng. Chem., Process Des. Dev. 13*, 248 (1974).
19. Hartman, M., Pata, J., and Coughlin, R. W., *Ind. Eng. Chem., Process Des. Dev. 17*, 411 (1978).